

Fission of super-heavy elements: ^{132}Sn -plus-the-rest, or ^{208}Pb -plus-the-rest ?

C. Ishizuka,^{1,*} X. Zhang,^{1,†} M.D. Usang,^{2,‡} F.A. Ivanyuk,^{1,3,§} and S. Chiba^{1,4,¶}

¹*Tokyo Institute of Technology, Tokyo, 152-8550 Japan*

²*Malaysia Nuclear Agency, Bangi, Malaysia*

³*Institute for Nuclear Research, 03028 Kiev, Ukraine*

⁴*National Astronomical Observatory of Japan, Tokyo, Japan*

(Dated: today)

In this work we try to settle down the controversial predictions on the effect of doubly magic nuclei ^{132}Sn and ^{208}Pb on the mass distributions of fission fragments of super-heavy nuclei. For this we have calculated the mass distribution of fission fragments of super-heavy nuclei from ^{274}Hs to $^{306}122$ within the dynamical 4-dimensional Langevin approach. We have found that in “light” super-heavies the influence of ^{208}Pb on the mass distributions is negligible small. In “heavy” super-heavies, $Z = 120 - 122$, the (quasi)symmetric peaks and strongly asymmetric peaks at fragment mass A_F close to $A_F = 208$ are of comparable magnitude to $A_F = 132 - 140$.

PACS numbers: 24.10.-i, 25.85.-w, 25.60.Pj, 25.85.Ca

Keywords: super-heavy elements, nuclear fission, mass distributions, double magic Sn-132 and Pb-208

I. INTRODUCTION

The physics of super-heavy elements (SHE) has a long history. The existence of the “island of stability” – the region of nuclei with the increased stability with respect to spontaneous fission – was predicted at the middle of 1960s. The possibility of closed shells at $Z = 114, N = 184$ was pointed out already in [1–3]. The systematic calculations in [4] within the macroscopic-microscopic method [5–7] for SHEs with the number of protons $106 < Z < 116$ have shown that many super-heavies are very stable, with the spontaneous fission half-lives of thousands of years or more. The highest fission barrier was predicted for a new double magic nucleus with $Z = 114$ and $N = 184$. Nevertheless, it took almost 30 years until the alpha-decay of the element with $Z = 114$ was observed experimentally at Flerov Laboratory for Nuclear Reactions in Dubna [8]. During the next two decades a lot of new experimental achievements were synthesized. The theoretical works were dedicated to the search of most favorable pairs of projectile and target and the excitation energy that would lead to the largest cross section of formation of evaporation residue – the super-heavy nucleus in its ground state.

With the development of experimental facility it became possible not only fix the fact of formation of SHE, but accumulate so many super-heavy nuclei that it turned out possible to examine their properties. One of the first property of interest – the process of fission of SHEs. For the successful planning and carrying out experiments it is very important to understand what kind

of fission fragments one should expect in the result of fission of SHE. On one side, it is clear that with increasing charge number Z of fissioning nucleus the Coulomb repulsion force grows and one could expect the symmetric mass distribution of fission fragments. One other side – the shell effects may still have a noticeable effect. The two double magic nuclei may contribute. The ^{132}Sn and ^{208}Pb have the shell correction to the ground state energy of the same magnitude. The ^{132}Sn plays a decisive role in formation of mass distribution of actinide and transactinide nuclei. In the experiment of Itkis group [9, 10] ^{132}Sn was found out as the light fragment of all investigated nuclei. The theoretical calculation within the scission point model [11] also predict ^{132}Sn (or slightly heavier) as the most probably light fragment for fission of SHE. At the same time there are few publications [12–15] where formation of heavy fragment close to ^{208}Pb is predicted as a main fission mode. In [16] the heavy fragment close to ^{208}Pb was obtained in the super-heavy region, $106 < Z < 114$.

In order to solve this contradiction and make it clear what kind of fission fragment mass distribution (FFMD) one could expect in the fission of SHEs, we have carried out the calculations of FFMD for a number of SHEs within the four-dimensional Langevin approach. We have found out the ^{208}Pb may appear as a supplementary heavy cluster in fission of Cn isotopes. With increasing charge number of SHEs the contribution of this heavy cluster became larger. For the element with $Z = 122$ the contributions of (almost) symmetric and strongly mass asymmetric ($A_F \approx 208$) are of the same magnitude. The details of calculations are given below.

II. THE MODEL

We describe the fission process within the Langevin approach [17], i.e., by solving the equations for the time evolution of the shape of nuclear surface of fissioning sys-

*Electronic address: chikako@nr.titech.ac.jp

†Electronic address: zhang.x.ba@m.titech.ac.jp

‡Electronic address: mark.dennis@nuclearmalaysia.gov.my

§Electronic address: ivanyuk@kinr.kiev.ua

¶Electronic address: chiba.satoshi@nr.titech.ac.jp

tem. For the shape parametrization we use that of two-center shell model (TCSM) [18] with 4 deformation parameters $q_\mu = z_0/R_0, \delta_1, \delta_2, \alpha$. Here z_0/R_0 refers to the distance between the centers of left and right oscillator potentials with $R_0 = 1.2A^{1/3}$, R_0 being the radius of spherical nucleus with the mass number A . The parameters δ_i , where $i = 1, 2$ describe the deformation of the right and left fragment tips. The fourth parameter α is the mass asymmetry and the fifth parameter of TCSM shape parametrization ϵ was kept constant, $\epsilon = 0.35$, in all our calculations.

The first order differential equations (Langevin equations) for the time dependence of collective variables q_μ and the conjugated momenta p_μ are:

$$\begin{aligned} \frac{dq_\mu}{dt} &= (m^{-1})_{\mu\nu} p_\nu, \\ \frac{dp_\mu}{dt} &= -\frac{\partial F(q, T)}{\partial q_\mu} - \frac{1}{2} \frac{\partial m_{\nu\sigma}^{-1}}{\partial q_\mu} p_\nu p_\sigma - \gamma_{\mu\nu} m_{\nu\sigma}^{-1} p_\sigma \\ &\quad + g_{\mu\nu} R_\nu(t), \end{aligned} \quad (1)$$

where the sums over the repeated indices are assumed. In Eqs.(1) the $F(q, T)$ is the temperature dependent free energy of the system, and $\gamma_{\mu\nu}$ and $(m^{-1})_{\mu\nu}$ are the friction and inverse of mass tensors and $g_{\mu\nu}$ is the random force.

The free energy $F(q, T)$ is calculated as the sum of liquid drop deformation energy and the temperature dependent shell correction $\delta F(q, T)$. The damping of shell correction $\delta F(q, T)$ with the excitation energy is described in detail in [19]. The single particle energies are calculated with the deformed Woods-Saxon potential [20, 21] fitted to the aforementioned TCSM shape parametrizations. It is to be noted the free energy is equal to potential energy at zero temperature.

The collective inertia tensor $m_{\mu\nu}$ is calculated within the Werner-Wheeler approximation [22] and for the friction tensor $\gamma_{\mu\nu}$ we used the wall-and-window formula, [23, 24].

The random force $g_{\mu\nu} R_\nu(t)$ is the product of white noise $g_{\mu\nu} R_\nu(t)$ and the temperature dependent strength factors $g_{\mu\nu}$. The factors $g_{\mu\nu}$ are related to the temperature and friction tensor via the modified Einstein relation,

$$g_{\mu\sigma} g_{\sigma\nu} = T^* \gamma_{\mu\nu}, \text{ with } T^* = \frac{\hbar\omega}{2} \coth \frac{\hbar\omega}{2T},$$

where T^* is the effective temperature [25]. The parameter ω is the local frequency of collective motion [25]. The minimum of T^* is given by $\hbar\omega/2$.

The temperature T in this context is related to the reaction energy E_x and the internal excitation energy E^* by,

$$E^* = E_{gs} + E_x - \frac{1}{2} m_{\mu\nu}^{-1} p_\mu p_\nu - V_{pot}(q, T=0) = aT^2,$$

where V_{pot} is the potential energy and a is the level density parameter. More details are given in our earlier publications, see [26–29]. Initially, the momenta p_μ

are set to be equal to zero, and calculations are started from the ground state deformation. Such calculations are continued until the trajectories reach the "scission point", which was defined as the point in deformation space where the neck radius reaches the value $r_{neck} = 1$ fm.

III. NUMERICAL RESULTS

In Fig. 1 we show the fission fragment mass distributions of super-heavy nuclei from ^{274}Hs to $^{306}\text{122}$ as function of fragment mass number A_F . As one can see, at $E_x = 30$ MeV the shell structure is washed out and all considered here nuclei fission symmetrically. At excitation energy $E_x = 10$ MeV the lighter superheavies Hs and Ds also undergo mass symmetric fission. The FFMDs of nuclei from ^{286}Cn to $^{306}\text{122}$ have three or four peak structure. Obviously, the multi-peak structure of FFMDs is the result of shell effects, which at $E_x = 10$ MeV are still large. The symmetric peak which in heavier

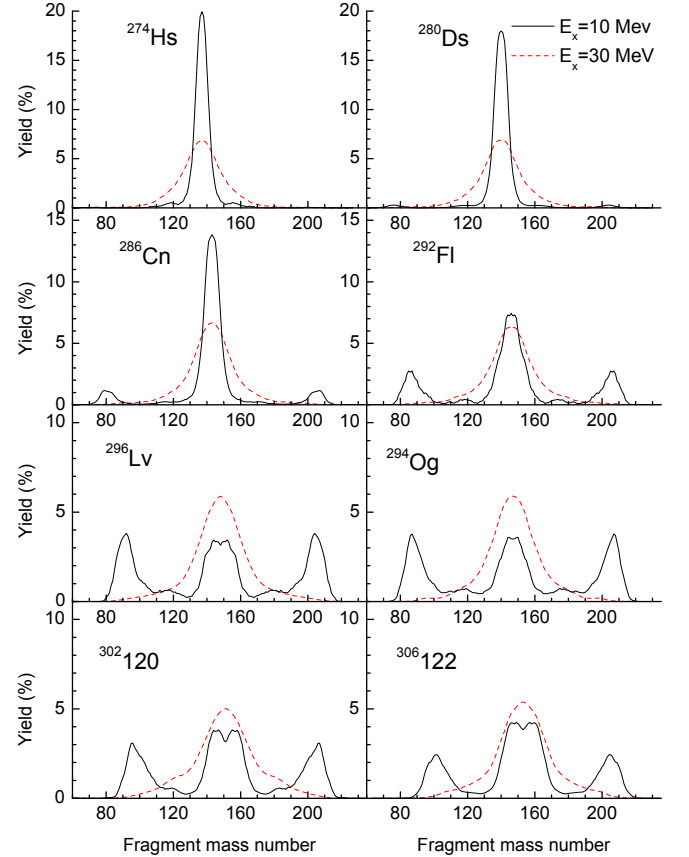


FIG. 1: The fission fragment mass distributions of super-heavy nuclei from ^{274}Hs to $^{306}\text{122}$ calculated for the excitation energy $E_x = 10$ MeV and $E_x = 30$ MeV as function of fragment mass number

SHEs is split into two components. The peaks of lighter fragments are located around $A_F = 140$.

One can also see the strongly asymmetric peak at the mass number close to $A_F = 208$. The strength of the (almost) symmetric and asymmetric components in FFMD of SHEs depends on the proton and neutron numbers of the compound nucleus. For ^{286}Cn the contribution of strongly asymmetric peak is very small. This contribution becomes larger for more heavy SHE. In the element $^{306}122$ the symmetric and mass asymmetric peaks are of the same magnitude.

In order to understand the reason of such complicated structure we have looked at the potential energy of fissioning nuclei. Fig. 2 shows the potential energy E_{def}

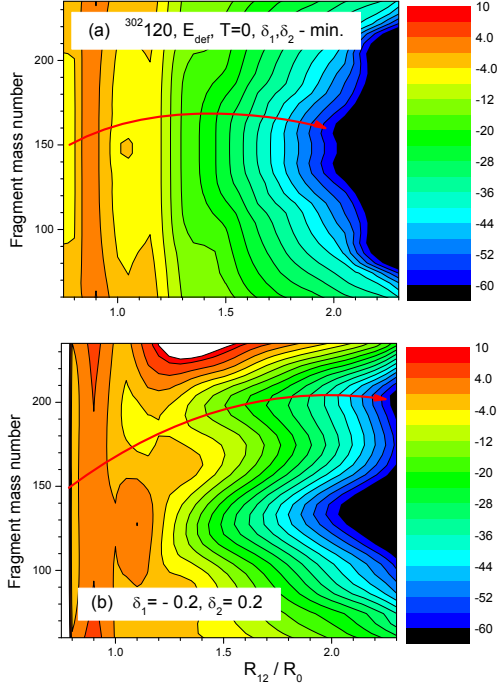


FIG. 2: (a) The potential energy of $^{302}120$ at $T = 0$ minimized with respect to deformation parameters δ_1 and δ_2 . (b) The potential energy of $^{302}120$ at $T = 0$ at fixed values $\delta_1 = -0.2$ and $\delta_2 = 0.2$.

of nucleus with $Z = 120$ and $A = 302$ at zero temperature as function of elongation (the distance R_{12} between left and right parts of nucleus) and mass asymmetry. In Fig.2(a) the energy was minimized with respect to the deformation parameters δ_1 and δ_2 . One clearly sees the bottom of potential energy leading to almost symmetric mass splitting. There is also a hint on the mass asymmetric valley at A_F close to $A_F = 208$. If the trajectories would follow the bottom of potential energy then the mass FFMD of $^{302}120$ would be mass symmetric. However it is well known that due to dynamical effects the trajectories may deviate substantially from the bottom of potential valley. We calculate the trajectories in four-dimensional deformation space. In this space there could be the local minima leading away from the bottom of potential valley. An example is shown in Fig. 2(b). Here we show the potential energy for fixed $\delta_1 = -0.2$ and

$\delta_2 = 0.2$.

One can see that in this subspace the trajectories can easily be trapped in the higher in energy valley leading to highly asymmetric fission. The trajectories can not skip into deeper symmetric valley because of barrier between these two valleys. In this way the strongly mass asymmetric peak appears in the mass distribution of fission fragments. In order to understand why this effects get stronger for heavier SHEs we have compared the dependence of potential energy close to the scission point, at $R_{12}/R_0 = 2.3$, on the mass asymmetry for two nuclei, ^{286}Cn and $^{306}122$, see Fig. 3.

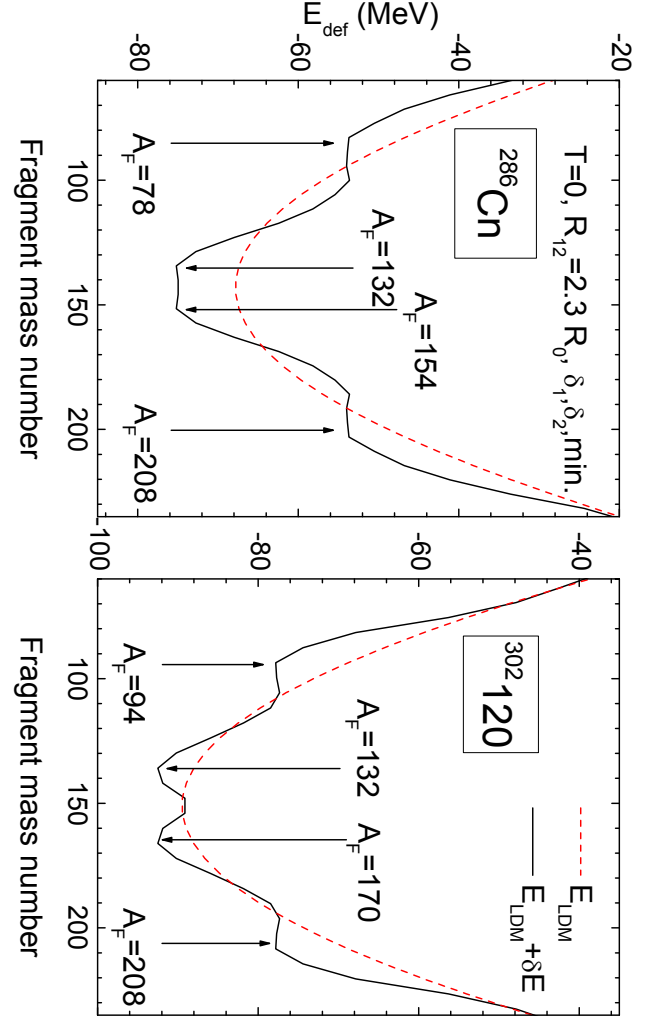


FIG. 3: The liquid drop (dash) and the total (solid) deformation energy near the scission line ($R_{12} = 2.3R_0$) for ^{286}Cn and $^{302}120$ as function of fragment mass number.

In Fig. 3 we compare the total deformation energies near the scission line for ^{286}Cn and $^{302}120$ with those of the liquid drop model. One can see that in case of ^{286}Cn the local minima corresponding to $A_F = 208$ and its paired fission fragment $A_F = 78$ are by 20 MeV higher than the minimum around $A_F = 132 - 154$. For $^{306}122$ the difference in almost symmetric and strongly mass

asymmetric minima is smaller, only 14 MeV. Thus in this case the trajectories have more chances to get into the mass asymmetric valley at $A_F = 208$ and its pair $A_F = 94$. As a result, the obtained FFMD becomes double mass asymmetric as seen in Fig. 1.

Another reason for the appearing of $A_F = 208$ contribution is the Z/A ratio. The Z/A ratio of fission fragment and of mother nucleus is approximately the same. For ^{132}Sn this factor is equal to 0.379, while for ^{208}Pb this ratio is equal to 0.394. The last ratio is much closer to that of ^{286}Cn and $^{306}122$ which are equal to 0.392 and 0.397 correspondingly.

In Fig. 4 we investigate the quadrupole deformation Q_{20} of the fragments, $Q_{20} = \langle r^2 Y_{20}(\cos \theta) \rangle$ from ^{236}U to $^{306}122$. The Q_{20} is the main measure of the deformation of fragment's shape. The negative Q_{20} corresponds to the oblate shape, the shape is spherical at $Q_{20} = 0$, and positive Q_{20} corresponds to the prolate shape. In actinides from ^{236}U to ^{259}Lr , there is no sign of ^{208}Pb shell. On the other hand, in SHEs from ^{274}Hs to $^{306}122$ one can clearly observe the $Q_{20}(A)$ distributions located in both $A_F = 132$ and 208, though we hardly see the peak at $A_F = 208$ of ^{274}Hs in the mass distribution shown in Fig. 1. Note that the averaged Q_{20} in actinides from ^{236}U to ^{257}Fm have positive Q_{20} in common, while the averaged Q_{20} in actinides from ^{258}Fm to ^{259}Lr commonly have $Q_{20} \simeq 0$. It means that deformed shell around $A_F = 132 - 140$ dominates the nuclear fission of actinides up to ^{257}Fm , though the spherical ^{132}Sn strongly affects the fission of actinides at and above ^{258}Fm . In the same way, in SHEs, we found that the fragments, with the mass number $A_F = 132 - 140$ are both deformed and of spherical shape with $Q_{20} \geq 0$, the fragments with $A_F = 208$, are spherical with $Q_{20} \approx 0$. In this manner, we can demonstrate that two spherical magicities at $A = 132$ and 208 play decisive roles in fission mechanisms.

Such results are quite reasonable because these fragments are nuclei with the double-closed shells. Another notable feature of $Q_{20}(A_F)$ plots is the difference of the distribution pattern between actinides (^{236}U to ^{259}Lr) and SHN (^{286}Cn to $^{306}122$). The $Q_{20}(A_F)$ distributions of actinides consist of two groups; the nearly spherical heavy fragments with $A_F = 132 - 140$ and the prolate light fragments. For the super-heavies from ^{286}Cn to $^{306}122$, we observe the spherical heavier fragments with the mass number around $A = 208$ and the complementary lighter fragments in addition to the mentioned above two groups seen in actinides.

In [29] we have noticed a very accurate correlation between the dependence of elongation of fragment and the multiplicity of prompt neutrons – the number of neutrons per fission event emitted from completely accelerated fragments. So, the averages values of Q_{20} (solid curves in Fig.4) represent actually the mass dependence of neutron multiplicity, what is an important observable of the fission process.

It should be pointed out that, in the experiment by Itkis group [9, 10] they found a peak around $A = 208$

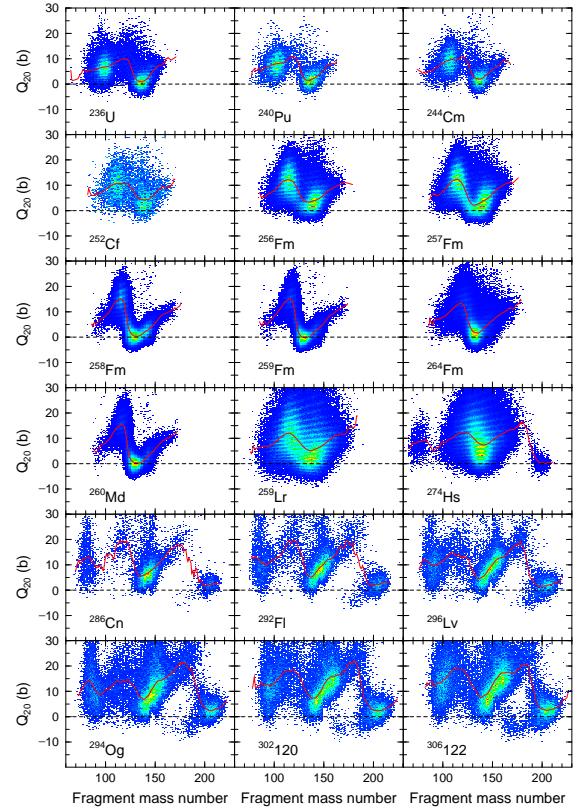


FIG. 4: The distribution of quadrupole deformation Q_{20} with respect to fission fragment mass number for nuclei from ^{236}U to $^{306}122$. The red curves mark the average values of Q_{20} .

and at complimentary light mass numbers. However, these peaks were assigned to be formed by quasi-fission process, not by fusion-fission. Such an interpretation is natural since the composite systems formed by hot-fusion reactions have excitation energy at least around 30 MeV, and the subtle shell effect, which gives rise to formation of the $A = 208$ and complimentary fragments, is washed out. Our calculation tells that only a small fraction of this peak can be indeed from fission of compound nucleus (indicating SHE was formed with slightly larger probability), but it is overwhelmed by the quasi-fission component so it cannot be identified in experiments. The only possibility that this supersymmetric fusion-fission component can be observed is after emission of a few prescission neutrons to cool the residues to excitation energy region down to around 10 MeV. If, e.g., multiplicities of prescission neutrons and fission fragments from corresponding residues are observed in coincidence, there is a chance that this supersymmetric component to be identified to come from fusion-fission events. It is highly desirable to have an experimental setup to distinguish these two components, namely, quasi-fission and fusion-fission, forming the same peaks.

IV. SUMMARY

Within the 4-dimensional Langevin approach we have calculated the mass distributions of fission fragments of super-heavy nuclei from ^{274}Hs to $^{306}122$. We have found a three-four peaks structure of mass distributions. In light super-heavies we see the dominant mass symmetric peak and small contributions from two highly asymmetric peaks at $A_H \approx 208$ and at the supplementary light fragment mass $A_L = A - 208$. With increasing mass of fissioning nuclei the symmetric peak splits into two components and the strongly mass asymmetric peaks become higher. For $^{306}122$ all four peaks in FFMD are approximately of the same magnitude. So, the answer to the question: “Fission of super-heavy elements: ^{132}Sn -plus-the-rest, or ^{208}Pb -plus-the-rest ? “ is: BOTH, the frag-

ment with the mass number close to ^{132}Sn , $A_F \approx 140$ plus the rest, and the fragment with the mass number $A_F \approx 208$ with spherical shape plus the rest.

Acknowledgments. This study comprises the results of “Research and development of an innovative transmutation system of LLFP by fast reactors” entrusted to the Tokyo Institute of Technology by the Ministry of Education, Culture, Sports, Science and Technology of Japan (MEXT) and KAKENHI Grant Number 18K03642 from Japan Society for the Promotion of Science (JSPS). One of us (F. I.) was supported in part by the project “Fundamental research in high energy physics and nuclear physics” of the National Academy of Sciences of Ukraine. We appreciate very much the useful discussions with Prof. N. Carjan and Prof. A.V. Karpov.

-
- [1] W.D. Myers and W.J. Swiatecki, Report UCRL-11980, (1965).
 - [2] A. Sobiczewski, F.A. Gareev, B.N. Kalitkin, Phys. Lett. **22**, 593 (1967).
 - [3] H. Meldner, Arkiv Fysik **36**, 593 (1967).
 - [4] S.G. Nilsson, C.F. Tsang, A. Sobiczewski, *et al*, Nucl. Phys. A **131**, 1 (1969).
 - [5] W.D. Myers and W.J. Swiatecki, Nucl. Phys. **81**, 1 (1966).
 - [6] V.M. Strutinsky, Nucl. Phys. A **95**, 420 (1967).
 - [7] V.M. Strutinsky, Nucl. Phys. A **122**, 1 (1968).
 - [8] Yu.Ts. Oganessian, A.V. Yeremin, A.G. Popeko, *et al*, Nature **400**, 242 (1999).
 - [9] M.G. Itkis, A.A. Bogatchev, I.M. Itkis, *et al*, J. Nucl. Rad. Sci. **3**, 57 (2002).
 - [10] M.G. Itkis, E. Vardaci, I.M. Itkis, G.N. Knyazheva, E.V. Kozulin, Nucl. Phys. A **944**, 204 (2015).
 - [11] N. Carjan, F.A. Ivanyuk, and Yu.Ts. Oganessian, Phys. Rev. C **99**, 064606 (2019).
 - [12] D.N. Poenaru, and R.A. Gherghescu, Phys. Rev. C **97**, 044621 (2018).
 - [13] M. Warda, A. Zdeb, and L.M. Robledo, Phys. Rev. C **98**, 041602(R) (2018).
 - [14] Z. Matheson, S.A. Giuliani, W. Nazarewicz *et al*, Phys. Rev. C **99**, 041304(R) (2019).
 - [15] G. Kaur, and M.K. Sharma, Nucl. Phys. A **990**, 79 (2019).
 - [16] M. Albertsson, B.G. Carlsson, T. Dossing *et al*, Preprint at <http://arXiv.org/nucl-th/1910.06030> (2019).
 - [17] Y. Abe, S. Ayik, P.-G. Reinhard, and E. Suraud, Phys. Rep. **275**, 49 (1996).
 - [18] J. Maruhn and W. Greiner, Zeit. f. Phys. **251**, 431 (1972).
 - [19] F.A. Ivanyuk, C. Ishizuka, M.D. Usang, and S. Chiba, Phys. Rev. C **97**, 054331 (2018).
 - [20] V.V. Pashkevich, Nucl. Phys. A **169**, 275 (1971).
 - [21] V.V. Pashkevich, Nucl. Phys. A **477**, 1 (1988).
 - [22] K.T.R. Davies, A.J. Sierk, J.R. Nix, Phys. Rev. C **13**, 2385 (1976).
 - [23] J. Blocki, Y. Boneh, J.R. Nix *et al*, Ann. Phys. **113**, 330 (1978).
 - [24] A.J. Sierk and J.R. Nix, Phys. Rev. C **21**, 982 (1980).
 - [25] H. Hofmann, D. Kiderlen, Int. Jour. Mod. Phys. E **7**, 243 (1998).
 - [26] M.D. Usang, F.A. Ivanyuk, C. Ishisuka, and S. Chiba, Phys. Rev. C **94**, 044602 (2016).
 - [27] C. Ishizuka, M.D. Usang, F.A. Ivanyuk, J.A. Maruhn, K. Nishio, S. Chiba, Phys. Rev. C **96**, 064616 (2017).
 - [28] M.D. Usang, F.A. Ivanyuk, C. Ishizuka, and S. Chiba, Phys. Rev. C **96**, 064617 (2017).
 - [29] M.D. Usang, F.A. Ivanyuk, C. Ishisuka, and S. Chiba, Scientific Reports **9**, 1525 (2019).